

# ❁ A $^{13}\text{C}$ -NMR Study of the Crystal Polymorphism and Internal Mobilities of the Triglycerides, Tripalmitin and Tristearin

S.M. BOCIEK, S. ABLETT and I.T. NORTON\*, Unilever Research, Colworth House, Sharnbrook, Bedfordshire, MK44 1LQ, England

## ABSTRACT

The combined NMR technique of cross-polarization, high power decoupling and magic angle spinning (CP/MAS) has been used in the study of the polymorphic forms of the two triglycerides, tripalmitin and tristearin. Variations in the  $^{13}\text{C}$  chemical shift values for the different polymorphic forms have been found and used to obtain molecular information, and to distinguish between chain orientations. Information on the relative mobilities of particular regions within the molecule for the different polymorphs also is presented.

## INTRODUCTION

Although the polymorphism of triglyceride molecules has been known for some time (1) and studied in detail by a number of physical techniques (2-7), there still is debate about the number of possible crystalline forms (8) and how the chains are organized within these crystals (9). The major problem with obtaining molecular information has been the difficulty in growing single crystals for detailed X-ray studies. To date, the only form for which this has been achieved, and the molecular structure characterized in any detail, is the highest melting  $\beta$ -polymorph (10).

The packing and molecular organization within the crystals of the lower melting point polymorphs have been studied mainly by X-ray powder diffraction techniques (11). This gives average information on the distances between distinct parts of the molecule but no detail on individual sites.

High resolution NMR (nuclear magnetic resonance) is a powerful technique for studying molecular conformation at individual sites but, until recently, this has been restricted to solution state studies. Typically, a broad line NMR spectrum is obtained for solids which gives information only on the overall motion of the molecules. However, an NMR technique recently has been developed, known as cross-polarization/magic angle spinning (CP/MAS), which allows high resolution  $^{13}\text{C}$ -NMR spectra to be obtained from solid materials (12). Spectra obtained by this technique can be analyzed, in a manner similar to those from solution state studies, to provide detailed information about the local environment and mobility of specific carbon sites within the molecule (13). A preliminary study has demonstrated how this technique can distinguish between the  $\alpha$ - and  $\beta$ -polymorphic forms of the pure triglycerides, tripalmitin and tristearin (14). In this paper, we report more extensive studies on these pure triglycerides to evaluate whether proposed crystal structures for the various polymorphs are viable (9,15,16).

## EXPERIMENTAL

### Materials

The samples of the purified mono-acid triglycerides were supplied by A.P.J. Mank of Unilever Research Laboratory Vlaardingen. The purity was checked by NMR, and gas chromatography of the fatty acid methyl esters. The tripalmitin was found to be >98% pure and the tristearin was >96% pure.

The different polymorphic forms of the triglycerides were obtained by heating samples to 95 C (above the known  $\beta$  melting point) for approximately 10 min. The

\*To whom correspondence should be addressed.

$\beta$ -form was produced by cooling slowly to room temperature, followed by reheating to 65 C, which was maintained for about 30 min. The  $\alpha$ -polymorph was obtained by rapidly cooling the heated sample. This was achieved by plunging a 1 g sample, contained within a thin walled glass tube, into an ethylene glycol bath at -20 C. The intermediate melting  $\beta'$ -form of tripalmitin was obtained by transferring the heated sample to a water bath controlled at 45 C  $\pm$  1 C until crystallization had occurred, usually within approximately 60 min. All attempts to produce a  $\beta'$ -form of tristearin proved fruitless. In each case, the polymorphic form was checked by X-ray diffraction measurements.

## METHODS

### Nuclear Magnetic Resonance

The  $^{13}\text{C}$ -NMR experiments were carried out on a Bruker CXP-300 NMR spectrometer, operating on a frequency of 75.46 MHz. A standard Bruker probehead was used for the CP/MAS studies, with an 'Andrews' design rotor of perdeuterated polymethyl-methacrylate (0.3 g of sample). Spectra were referenced to the residual signal from the rotor at 44 ppm relative to a TMS (tetramethylsilane) standard. The experimental conditions used were: a single contact pulse of 5 ms, a rotor frequency of 3.8 KHz and spinlocking and decoupling fields of 50 KHz. Data were collected with a spectral width of 30 KHz, an acquisition time of 135 ms and a recycle delay of 20 s (3-4 times the longest proton  $T_1$  of the solid). Two hundred scans were accumulated per spectrum. The probe used had no temperature control, hence the temperature for all spectra was ambient (approximately 298 K). The interrupted-decoupling spectra (17) were recorded by switching off the decoupler for a period of 68  $\mu\text{sec}$  between the end of the contact pulse and the beginning of the data acquisition. The 'magic angle' was adjusted for each sample by maximizing the spinning side bands of the  $^{79}\text{Br}$  resonance for KBr, which was a separate solid layer at the base of the rotor.

The liquid state spectra were obtained with a standard high resolution probehead (10 mm sample tube) at 353 K. Broad-band gated decoupling was used to suppress the nuclear overhauser effect. Purity checks by NMR were carried out in  $\text{CDCl}_3$  solutions and were based on the method of Pfeffer (18).

### X-ray Diffraction

X-ray diffraction measurements were carried out using a Philips constant potential generator, producing  $\text{CuK}\alpha$  radiation ( $\lambda = 0.154 \text{ nm}$ ), and an Anton Paar TTK camera. Diffraction was measured with a proportional counter, and the temperature control of the samples (dimension 14 mm  $\times$  10 mm  $\times$  1 mm) was by a Haake F3/K circulatory bath. The angular range was scanned at a rate of 1 deg/min.

## RESULTS AND DISCUSSION

NMR spectroscopy has been used to obtain spectra of both the liquid and crystalline states of the two triglycerides, tripalmitin and tristearin. A comparison of the liquid (18) and solid state spectra (14) allows the peaks in the solid

TABLE I

Comparison of the Observed Liquid and Solid State Chemical Shifts for Tripalmitin<sup>a</sup>

Group	Carbon	Chemical shift			
		Liquid	Solid state		
			$\alpha$ -polymorph	$\beta'$ -polymorph	$\beta$ -polymorph
Glycerol	1'	61.9	61.9	64.9	59.6
	2'	68.8	67.4	68.8	67.8
	3'	61.9	61.9	64.9	61.2
Carbonyl	Chain 1			173.3	173.4
	Chain 2	172.7	171.9	172.5	172.9
	Chain 3			173.3	174.6
Methyl	16	13.9	14.0	14.3	15.5
Main hydrocarbon chains	2	33.9	33.8	34.0	35.3
	3	25.0	26.0	26.1	27.0
	4-13	~29.5	32.7	32.8	34.0
	14	31.8	33.8	34.0	35.3
	15	22.5	24.1	23.9	25.5

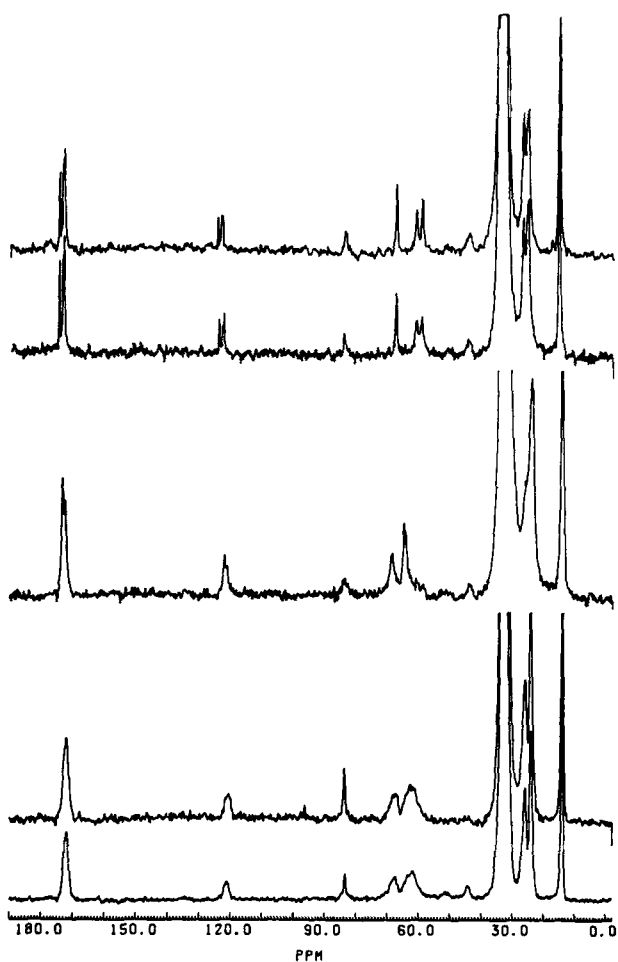
<sup>a</sup>Values reported are the peak centers.

FIG. 1. NMR spectra obtained for the different polymorphic forms of the two triglycerides. A,  $\beta$ -form tristearin; B,  $\beta$ -form tripalmitin; C,  $\beta'$ -form tripalmitin; D,  $\alpha$ -form tristearin, and E,  $\alpha$ -form tripalmitin. The peaks at 44 ppm are the residual signal from the rotor, and the peaks at 121 and 84 ppm are spinning side bands from the carbonyl and main chain  $\text{CH}_2$  regions, respectively.

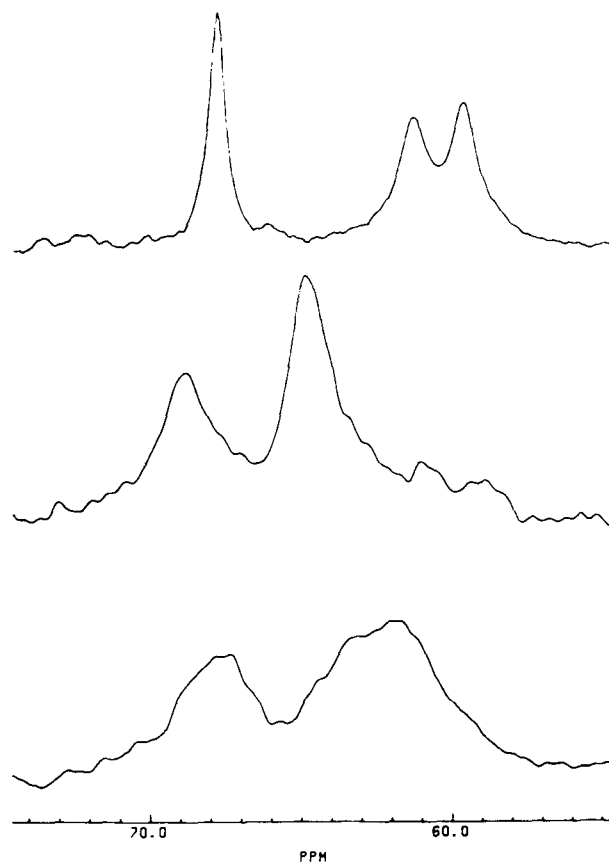


FIG. 2. Expanded chemical shift plot of the glycerol region of the NMR spectra obtained for the three polymorphic forms of tripalmitin  $\alpha$ -form (lower curve),  $\beta'$ -form (middle curve) and  $\beta$ -form (upper curve).

## POLYMORPHISM AND MOBILITY

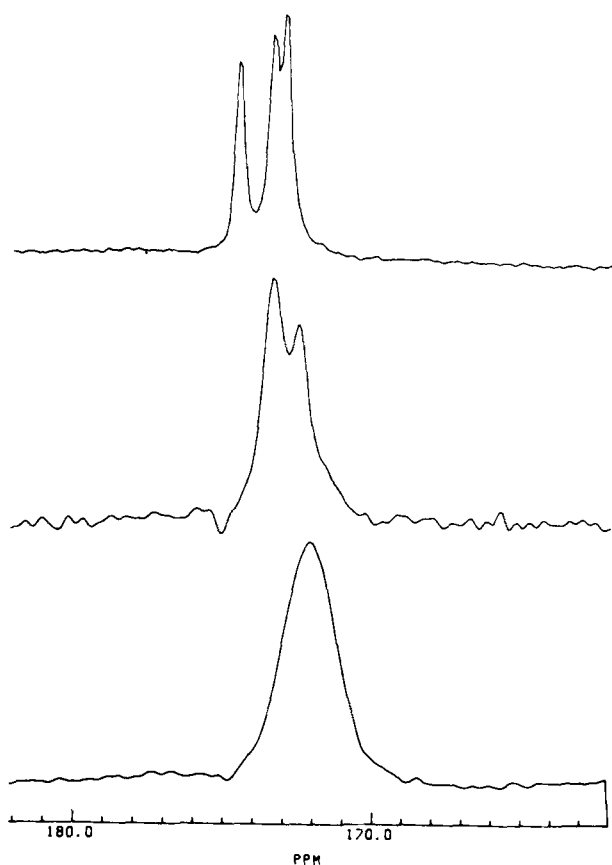


FIG. 3. Expanded chemical shift plot of the carbonyl region of the NMR spectra obtained for the three polymorphic forms of tripalmitin (order as in Fig. 2).

state to be assigned (Table I). Other points to note (Fig. 1) are the peaks in the solid state spectrum due to spinning side bands (84 and 121 ppm) and residual peaks from the rotor material (44 ppm). It is apparent from these spectra that the inherent linewidths for the solid are much larger than those observed for the liquid. As suggested by Shaeffer and Stejskal (19), this extra linewidth probably is caused by a distribution of isotropic chemical shifts due to a number of possible non-interchangeable environments for each carbon atom. The three polymorphic forms of tripalmitin and the  $\alpha$ - and  $\beta$ -forms of tristearin were produced by the method outlined in the Materials and Methods section. The spectra obtained for the two triglycerides (Fig. 1) in each of the polymorphic forms were identical, but distinct differences were observed among the three polymorphs  $\alpha$ ,  $\beta'$  and  $\beta$ . An interesting observation is that the chemical shift differences are large compared with those normally observed in the liquid state. For example, the methyl carbons of liquid triglycerides typically occur in the range of 13.8 to 14.2 ppm, while for the  $\beta$ -form of tripalmitin and tristearin they were found to be at 15.5 ppm.

In order to demonstrate specific features of the spectra more clearly, the glycerol head group region (55-75 ppm) is shown in Figure 2, the carbonyl region (162-182 ppm) in Figure 3 and the methyl and methylene region (10-40 ppm) in Figure 4. In the glycerol region it can be seen that for the  $\alpha$ -polymorphic form, two broad peaks are observed with the areas integrating to give a 2:1 ratio. The general picture is, therefore, probably very similar to the liquid state in which the 1 and 3 positions of the glycerol are equivalent.

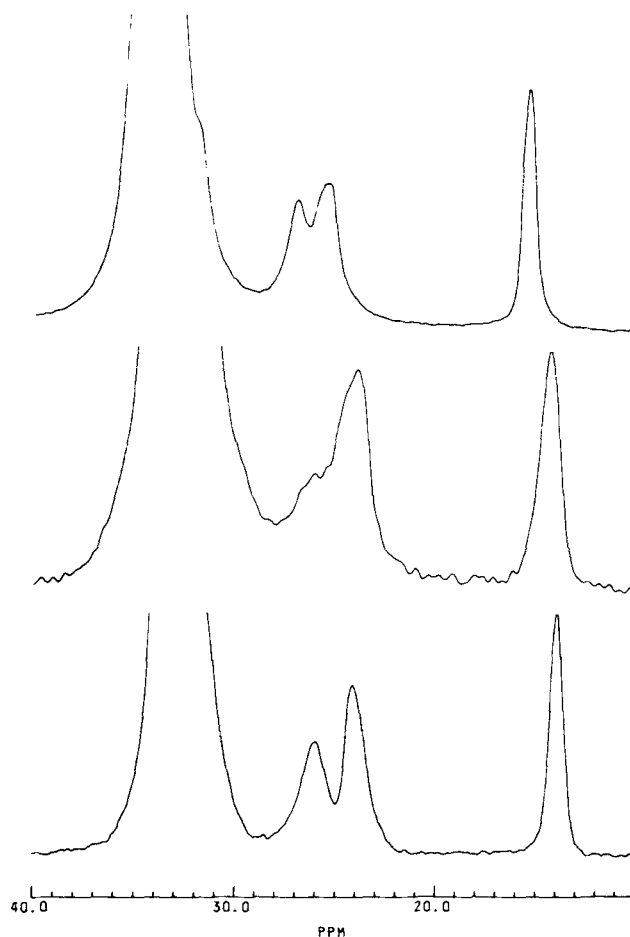


FIG. 4. Expanded chemical shift plot of hydrocarbon region of the NMR spectra obtained for the three polymorphic forms of tripalmitin (order as in Fig. 2).

The broadness of these peaks probably is due to molecules experiencing different environments. This observed broadness and the 2:1 ratio of the peak areas is in agreement with the proposed molecular organization of this form (9).

In the spectra obtained for the  $\beta$ -polymorph the glycerol carbons are observed to have shifted to higher field than for the same carbons in the  $\alpha$ -form, indicating an increased shielding from the magnetic field. It is also found that the three glycerol carbon resonances are resolved into individual peaks of equal area. This shows that the carbons at the 1 and 3 positions in the glycerol are no longer equivalent and hence experience some form of an asymmetric environment.

The overall upfield shift of the glycerol carbons in the  $\beta$ -form probably occurs as a consequence of the increased order within this crystal form which allows a greater interaction between the triglyceride molecules. The observed non-equivalence of the 1 and 3 positions of the glycerol carbons results from the position and orientation of the carbonyl dipole. Using this as the major consideration in conjunction with molecular models (Fig. 5) and using the packing arrangements reported (10), the peak centered about 59.6 ppm can be assigned to the carbon in the linear position. Thus, the peak centered at 61.2 ppm is assigned to the glycerol carbon which has side chain character (referred to as position 3 in the rest of this paper).

In the  $\beta'$ -form the whole of the glycerol region has shifted to lower field than observed for either the  $\alpha$ - or  $\beta$ -forms. The 1 and 3 peaks are again unresolved and appear as a single peak centered at 64.9 ppm. The two small peaks

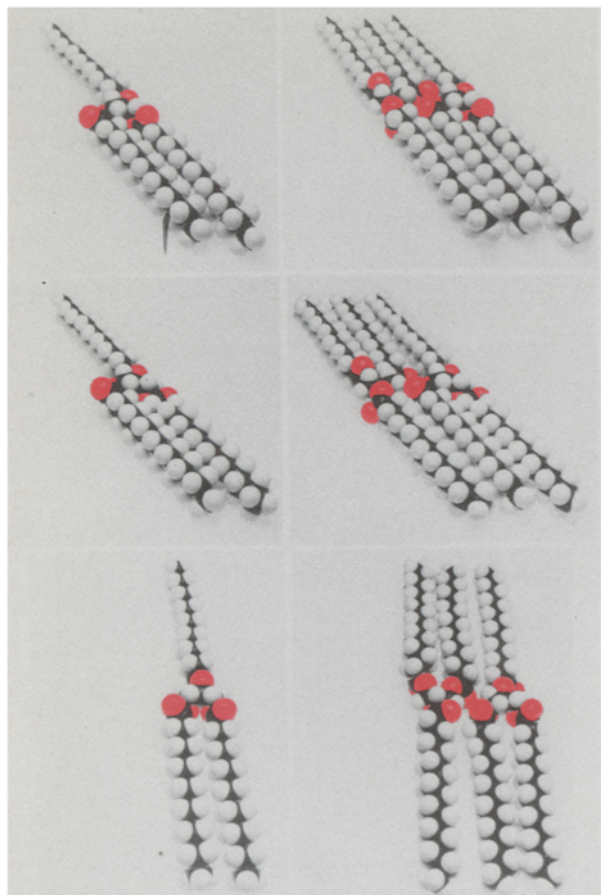


FIG. 5. Molecular models of  $\alpha$ - (lower),  $\beta'$ - (middle) and  $\beta$ - (upper) forms of tripalmitin.

centered about 59.6 and 61.2 ppm observed in this sample suggest some  $\beta$ -crystals were present. This was confirmed by X-ray diffraction data with similar amounts of the  $\beta$ -polymorph observed by both techniques. An advantage of having this impurity is that it can be used as an internal reference to demonstrate that the chemical shift differences between the different crystalline forms are real.

The 2:1 ratio of the glycerol carbons shows that there is again symmetry in this region, while the overall shift downfield can be explained by rotations about the glycerol carbon to oxygen bonds of the fatty acid chains to give a structure (20) with alternating perpendicular chains. There is likely to be less intermolecular interactions in this structure than found in the  $\beta$ -form which probably causes a deshielding of the glycerol carbons and hence the general downfield shift in peak position.

The chemical shift changes and the linewidth information obtained on the glycerol carbons is observed to be mirrored in the carbonyl carbons (Fig. 3). For the  $\alpha$ -polymorph, the physical environments of the carbons from the carbonyls of the individual chains are so similar that a single unresolved peak is observed at 171.9 ppm.

In the  $\beta$ -form a peak from each of the three carbonyl carbons was observed (Fig. 3) along with a general downfield shift of this region. Taken with the upfield shift of the corresponding glycerol carbons, this is consistent with a weakening of the carbonyl dipole due to a delocalization of electron density caused by intermolecular overlap of the non-hybridized p-orbitals. Considering the known (10) molecular packing in the  $\beta$ -form, we assign the low field peak at 174.6 ppm to the fatty acid chain in position 3.

For the  $\beta'$ -structure, the carbonyl peaks shift downfield

from those observed from the  $\alpha$ -form, but have shifted to a lesser extent than with the  $\beta$ -form. As can be seen in Figure 3, there appear to be two peaks which are not well resolved. A derivative least squares fitting routine employing Lorentzian line shapes was used to analyze this region of the  $\beta'$ -spectrum. The best fit was when the peak areas had approximately a 2:1 ratio. The peak at higher field was from a single carbon, and the other peak at lower field was from two unresolved carbons at approximately the same chemical shift value as the carbonyl carbons in the linear portion of the molecule in the  $\beta$ -polymorphic form.

The rotations about the hydrocarbon chain carbon to oxygen bond, discussed above, may explain the differences observed for the carbonyl carbons. Such rotations would disrupt part of the intra- and intermolecular interaction possible in the  $\beta$ -polymorph, thus explaining the intermediate chemical shift values observed for the  $\beta'$ -form. Also, such a rotation would cause the carbonyls of the fatty acid at positions 1 and 3 to be in very similar environments and thus result in the observed single peak for these carbons.

The methyl carbons appear as a single peak for all three polymorphic forms (Fig. 4), with the  $\alpha$ - and  $\beta'$ -forms having approximately the same chemical shift value of 14 ppm and the  $\beta$ -form a value of 15.5 ppm. Corresponding spectral differences were observed for the main chain  $\text{CH}_2$  resonances. Similar results have been reported by Vanderhart (21) for a series of different chain length alkanes, which were interpreted in terms of the same type of change in crystal packing as reported (22) for the different polymorphic forms of the triglycerides.

#### Molecular Motion

There have been a number of proposals on the amount of retained mobility in the  $\alpha$ -form (8,14), and also on the way in which this mobility is retained with models proposed in which a single chain retains a substantial amount of rotational freedom (8) or where liquid like methyl end group regions exist (23). These disagreements have arisen from the lack of a direct method of measuring the mobilities. It is now possible, however, to gain information about the relative mobilities of different regions of the triglyceride molecules by a modified version of the CP/MAS technique (known as 'interrupted decoupling'). This involves switching off the decoupler for a short period of time (typically approximately 50  $\mu\text{s}$ ) between the end of the contact pulse and the start of the signal acquisition. During this time, the  $^{13}\text{C}$  magnetization is dephased due to static  $^{13}\text{C}$ - $^1\text{H}$  dipolar coupling. However, if there is motion present this coupling is reduced. The result is that the signal from mobile protonated carbons will be only partially suppressed. It should be noted that any non-protonated carbons also give rise to signal even if they are immobile.

A standard CP/MAS spectrum and an interrupted decoupling spectrum for the  $\alpha$ -polymorphic form of tripalmitin are compared in Figure 6. As discussed, the peak from the carbonyl carbons appears as normal in the interrupted-decoupling spectrum. The majority of the intensity of the methyl peak also is observed, suggesting that the ends of the chains are very mobile. In contrast, the glycerol carbons are completely absent, and only a small amount of signal is observed from the carbons in the main hydrocarbon chains.

A comparison of the interrupted decoupling and the standard CP/MAS spectra for the three polymorphic forms of tripalmitin revealed that in each form the peak from the carbonyl carbon appeared unchanged in the interrupted spectrum. The glycerol carbons were absent for all three forms, as was the peak from the carbon at C3 (i.e. 26.5 ppm) which shows that, in all three polymorphs, there is

## POLYMORPHISM AND MOBILITY

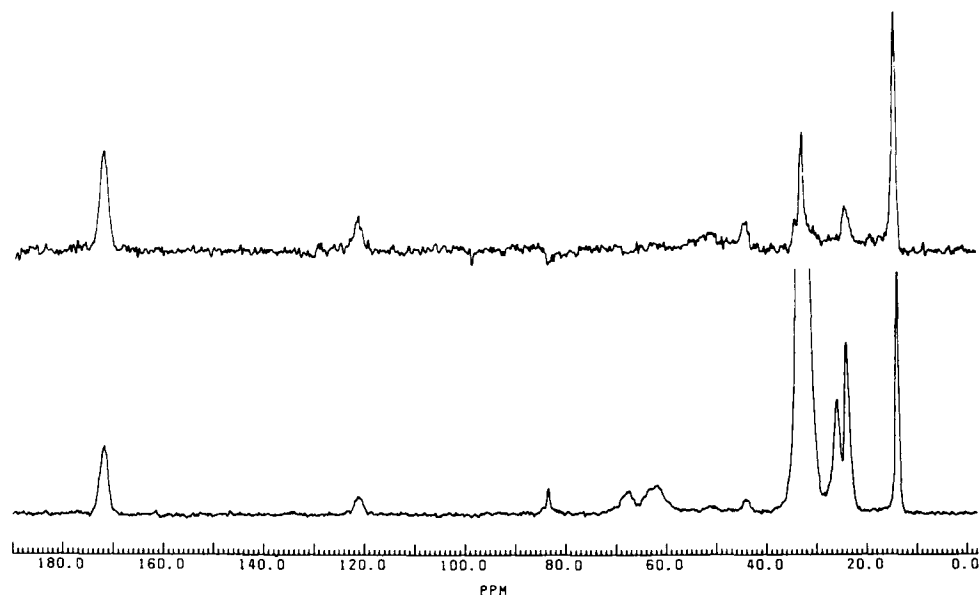


FIG. 6. Comparison of the standard CP/MAS (lower curve) and interrupted-decoupling  $^{13}\text{C}$  NMR spectra obtained for the  $\alpha$ -form of tripalmitin.

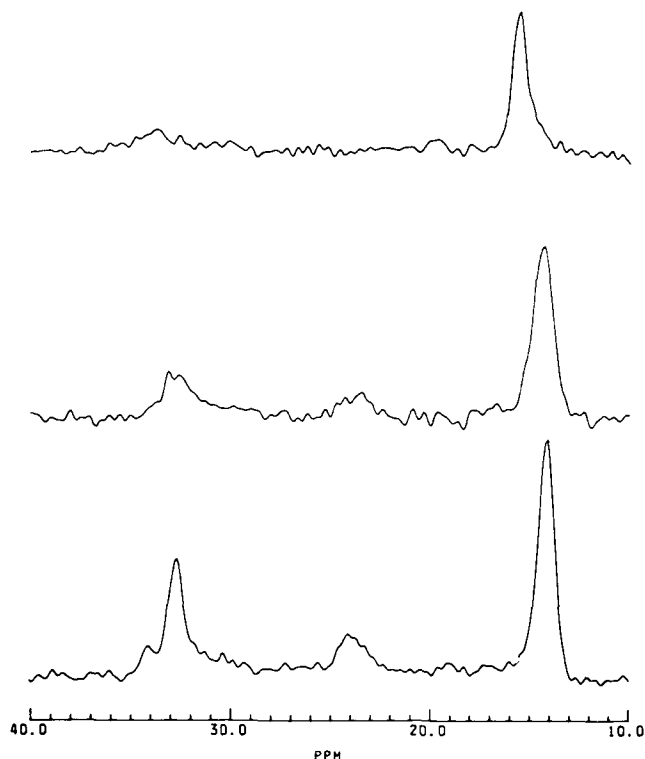


FIG. 7. Interrupted-decoupling spectra obtained for tripalmitin in the  $\alpha$  (lower curve),  $\beta'$  (middle curve) and  $\beta$  (upper curve) polymorphic forms.

little mobility in the center of the molecule. The interrupted decoupled spectra of the methyl and main chain carbon regions (10-40 ppm) are compared in Figure 7. It can be seen that the amount of main chain  $\text{CH}_2$  signal observed (at approximately 33 ppm) is much lower for the  $\beta$ -form than the  $\beta'$ -polymorph, and both are smaller than the observed signal from the  $\alpha$ -form. The methylene at approximately 24 ppm ( $\text{C}_{15}$ ) and the methyls follow the same trend. These results suggest that the retained mobility within the triglyceride molecules is at the ends of the hydrocarbon chains, as previously proposed for the  $\alpha$ -form

(23), and that there is more overall mobility in the  $\alpha$ -form than either the  $\beta$ - or  $\beta'$ -forms. The small amount of  $\text{CH}_2$  observed for the  $\alpha$ -polymorph is consistent with our previous conclusion from statistical thermodynamics (14) that one chain does not retain a large amount of mobility.

The same comparison was made between the  $\alpha$ - and  $\beta$ -polymorphs of tristearin. Here the  $\beta$ -form shows more relative mobility than the corresponding tripalmitin spectrum, which probably is a consequence of the longer chain length. In all other respects, the results were the same as observed for tripalmitin.

The results obtained by these new NMR techniques are in good agreement with the proposed molecular structures. The differences observed among the three polymorphic forms are consistent with the proposed rotations in the glycerol head group. The interrupted decoupling studies show that although the  $\alpha$ -polymorphic forms have more molecular mobility than either the  $\beta'$ - or  $\beta$ -forms, this is retained mainly at the methyl ends of the chain. Also, it is apparent that the methyls in the  $\beta$ -polymorphic forms retain mobility.

## ACKNOWLEDGMENTS

C. D. Lee-Tuffnell made the X-ray measurements, and P. J. Lillford and N. A. Kitchen provided helpful advice and discussion.

## REFERENCES

1. Clarkson, C.E., and T. Malkin, *J. Chem. Soc.* 666 (1934).
2. Chapman, D., *Chem. Rev.* 62:433 (1962).
3. Lutton, E.S., and A.J. Fehl, *Lipids* 5:90 (1970).
4. Hannewijk, J., and A.J. Haighton, *JAOCS* 35:457 (1958).
5. Chapman, D.J., R.E. Richards and R.W. Yorke, *Chem. Soc.* 436:444 (1960).
6. Baily, A.E., and G.D. Oliver, *Oil and Soap* 21:300 (1944).
7. Friedman, M., H.L. Rosano and J.H. Whittam, *J. Coll. Int. Sci.* 40:123 (1972).
8. Hagemann, J.W., and J.A. Rothfus, *JAOCS* 60:1123 (1983).
9. Hagemann, J.W., and J.A. Rothfus, *JAOCS* 60:1308 (1983).
10. Larsson, K., *Ark. Kemi.* 23:1 (1965).
11. Hoerr, C.W., and F.R. Paulicka, *JAOCS* 45:793 (1968).
12. Schaefer, J., E.O. Stejskal and R. Buchdahl, *Macromolecules* 8:291 (1975).

13. Wehrli, F.W., and T.W. Wirthlin, Interpretation of Carbon-13 NMR Spectra, Heyden & Son Ltd., London (1976) pp. 64-150.
14. Norton, I.T., C.D. Lee-Tuffnell, S. Ablett and S.M. Bociek, JAOCS 62:1237 (1985).
15. Lutron, E.S., JAOCS 49:1 (1972).
16. De Jong, S., and T.C. van Soest, Acta Cryst. 34:1570 (1978).
17. Opella, S.J., and M.H. Frey, JACS 101:5854 (1979).
18. Pfeffer, P.E., F.E. Luddy, J. Unruh and J.N. Shoolery, JAOCS 54:380-386 (1977).
19. Schaefer, J., and E.O. Stejskal, Topics in Carbon-13 NMR Spectrosc. 3:283 (1980).
20. Hagemann, J.W., and W.H. Tallent, JAOCS 49:118 (1972).
21. Van der Hart, D.L., J. Mag. Reson. 44:117-125 (1981).
22. Chapman, D., The Structure of Lipids, Methuen & Co. Ltd., 1965.
23. Hernqvist, L., and K. Larsson, Fette, Seifen, Anstrichm. 9:349 (1982).

[Received February 19, 1985]

## ✿ Isolation and Chemical Investigation of Teak (*Tectona grandis* Linn) Seed Proteins

S. LASKAR\*, S. GHOSH MAJUMDAR and B. BASAK, Natural Product Laboratory, Chemistry Department, The University of Burdwan, Burdwan 713104, West Bengal, India

### ABSTRACT

Proteins were extracted from the deoiled seeds of *Tectona grandis* Linn., Fam. Verbenaceae, a quality lumber source, in aqueous solutions of various pH's or by different concentrations of NaCl at pH 8.0. Chemical analysis of isolated protein identified 15 amino acids, of which eight were essential. Gel filtration on Sephadex G-200 revealed the presence of six components, whose molecular weights were determined by two comparable standard methods. Seven components were resolved electrophoretically (SDS-PAGE electrophoresis) and their molecular weights were found to be 118,900, 92,300, 72,400, 62,400, 43,600, 39,800 and 32,400.

### INTRODUCTION

Teak (*Tectona grandis* L.) is a species of a small genus *Tectona* belonging to the family Verbenaceae. It enjoys a worldwide reputation as a quality lumber resistant to attack by termites (1). It is generally used in aesthetic crafts and is widely cultivated in tropical countries. This plant is indigenous to India, Burma and the western part of Thailand (2). Handling of its wood causes contact dermatitis (3), and different parts of the plant are used as medicines.

The seed kernel contains 40% oil (4), and the total seed only 7.3%. Seed oil may be used for edible purposes (5) and contains no unusual fatty acids. In addition to oil, the seed kernel contains a high concentration of protein (4). The seed protein and oil have not been used extensively until now, although a small amount of oil has been used in remote villages of India to prevent falling of hair (2). Recently, it has been observed that the seed protein is well tolerated by albino rats (6).

This report summarizes the extraction (7) and isolation of protein from deoiled Teak seed, the amino acid composition of isolated protein and determination of molecular weights of its different fractions by gel filtration and by sodium dodecyl sulphate (SDS) polyacrylamide gel electrophoresis.

### EXPERIMENTAL PROCEDURE

#### Materials

All reagents used in this investigation were of analytical grade. Reagents for SDS-Polyacrylamide gel electrophoresis, Sephadex G-200 (for gel filtration) and proteins used for standard calibration (BSA, Ovalbumin, Pepsin and Lysozyme) were purchased from Sigma Chemical Co., St. Louis, Missouri.

\*To whom correspondence should be addressed.

### Extraction of Proteins from Teak Seed

Finely powdered teak seeds were extracted with petroleum ether (40-60°) in a Soxhlet for 48 hrs. Then the seeds were washed well with acetone and air dried. The nitrogen content of the seed was estimated by the micro-Kjeldahl method (8) and the protein content was determined (9).

Extraction of proteins (7) from deoiled seeds was carried out using 20 volumes (w/v) of extractant at room temperature for 30 min, either at various pH's (2-12) or by using gradient NaCl solution (2-10%) at pH 8.0. The nitrogen content of each extract was monitored by the micro-Kjeldahl method (9).

### Determination of Amino Acid Composition of Teak Seed Protein

The deoiled teak seed was stirred with 20 volumes (w/v) cold aqueous 4% sodium chloride solution at pH 10-11 (adjusted by adding 0.5M sodium hydroxide solution) for one hour. It was then centrifuged at 5000 RPM for 10 min, and the suspension was filtered through Whatman No. 1 filter paper. The protein solution was dialyzed against distilled water and freeze dried. The resulting protein product was deep brown in color.

Acid hydrolysis of the seed protein was conducted by hydrolyzing freeze dried sample with 3 ml 6 (N) HCl, containing 5% thioglycolic acid (10), in a sealed evacuated tube at 110 C for 24 hr. Amino acid composition of the hydrolysate was determined using a Beckman Multichrome 4255 amino acid analyzer.

### Preparation of Protein Sample and Gel Filtration on Sephadex G-200

For gel filtration, the protein was extracted with 4% NaCl at pH 8.0 and was dialyzed against 0.01M phosphate buffer (pH 7.2) for 48 hr at 4 C. The protein was obtained by freeze drying the dialyzed solution. Then it was dissolved in 0.01M phosphate buffer (pH 7.0) containing 0.2M NaCl to obtain a protein concentration of 4 mg/ml.

Gel filtration (11) of teak seed proteins on Sephadex G-200 was conducted on a 2.5 x 40 cm column at 25 C. 1.5 ml of the protein sample was applied to the top of the gel bed. The eluting buffer was 0.01M sodium phosphate (pH 7.0) containing 0.2M NaCl. Fractions of 2 ml were collected at the rate of 0.4 ml/min and monitored at 280 nm. The molecular weights of the components corresponding to the peaks A, B, C, D, E and F (Fig. 1) were determined from a linear plot ( $V/V_0$  against log mol wt, Fig. 2) and calibrated with reference protein standards